Eurasian Journal of Analytical Chemistry
ISSN: 1306-3057 OPEN ACCESS 2025 20(2): 143-150

# "Synthesis And Characterization Of Novel Adsorbents And Their Utilization For Multifarious Applications"

**Rane D.**, Sikarwar A.K *** ,Choubey O.N.** and Nirapure E.***

***Govt Home Science College, Narmadapuram (M.P.)
**PMCoE Govt Narmada Post Graduate College, Narmadapuram (M.P.)
*PMCoE J H Govt P G College, Betul (M.P.)

***Correspondence Author:** durgesh10rane10@gmail.com

**Abstract**:
This research presents the development, characterization, and application of novel adsorbent materials based on modified agricultural waste biomass and synthetic composites. Three distinct adsorbent types were synthesized: (1) functionalized rice husk biochar (FRHB), (2) magnetic chitosan-graphene oxide nanocomposite (MCGN), and (3) hierarchical zeolite-based metal-organic framework (HZMOF). These materials were extensively characterized using SEM, FTIR, XRD, TGA, BET, and zeta potential measurements. Adsorption studies revealed exceptional performance for heavy metal removal ($Pb^{2+}$, $Cd^{2+}$, $Cr^{6+}$), organic dye elimination (methylene blue, Congo red), and pharmaceutical contaminant sequestration (diclofenac, ibuprofen). The maximum adsorption capacities reached 245.8 mg/g for $Pb^{2+}$ (HZMOF), 198.4 mg/g for methylene blue (MCGN), and 156.7 mg/g for diclofenac (FRHB). Kinetic and isotherm studies indicated that adsorption followed pseudo-second-order kinetics and the Langmuir isotherm model. Thermodynamic investigations confirmed the spontaneous and endothermic nature of the adsorption processes. The adsorbents demonstrated remarkable reusability over five cycles with minimal capacity loss. This research contributes significantly to sustainable remediation technologies by developing cost-effective, high-performance adsorbents from renewable resources with multifarious environmental applications.

**Keywords:** *Novel adsorbents; Heavy metal removal; Dye adsorption; Pharmaceutical contaminants; Sustainability*

## 1. Introduction

Environmental pollution from heavy metals, organic dyes, and emerging contaminants poses significant threats to ecosystems and public health globally (Mahmood et al., 2020). Conventional water treatment technologies often fall short in efficiently removing these diverse.
Pollutants, particularly at low concentrations (Sarker et al., 2022). Adsorption has emerged as a preferred remediation technique due to its simplicity, effectiveness, and economic viability (Thakur & Thakur, 2021). The development of specialized adsorbents with enhanced selectivity, capacity, and renderability represents a critical frontier in environmental remediation research.

Recent advances in materials science have facilitated the design of novel adsorbents with tailored properties for specific contaminants (Li et al., 2019). Biomass-derived adsorbents offer a sustainable approach by valorizing agricultural waste while providing cost-effective solutions for environmental cleanup (Shah et al., 2021). Concurrently, nanocomposites combining magnetic properties with high surface area materials enable efficient separation after adsorption processes (Kausar et al., 2018). Metal-organic frameworks (MOFs) have similarly garnered attention for their exceptional porosity and tunable functionalities (Kumar et al., 2019). Despite these advancements, significant challenges persist in developing adsorbents that simultaneously address multiple contaminant classes while maintaining economic viability and sustainability (Wang et al., 2020). The integration of various materials into multifunctional composites presents a promising direction for enhancing adsorption performance across diverse pollutant types (Zhang et al., 2022).

This research addresses these challenges by synthesizing and characterizing three novel adsorbent materials: (1) functionalized rice husk biochar (FRHB), which utilizes abundant agricultural waste; (2) magnetic chitosan-graphene oxide nanocomposite (MCGN), combining magnetic separability with high adsorption capacity; and (3) hierarchical zeolite-based metal- organic framework (HZMOF), leveraging the strengths of both zeolites and MOFs. These materials were comprehensively evaluated for their effectiveness in removing heavy metals, organic dyes, and pharmaceutical contaminants from aqueous solutions.

The study aims to (i) develop efficient synthesis protocols for each adsorbent type, (ii) characterize their physicochemical properties using advanced analytical techniques, (iii) evaluate their adsorption performance across

multiple contaminant classes, (iv) Elucidate the underlying adsorption mechanisms, and (v) assess their reusability for practical applications.
The findings contribute to the development of sustainable remediation technologies with potential industrial applications.

## 2. Materials and Methods

### 2.1 Materials

For the experiment Rice husks were obtained from a local rice mill in Narmadapuram district Madhya Pradesh, India. Chitosan (medium molecular weight, 75-85% deacetylated), graphite powder, ferric chloride hexahydrate ($FeCl_3.6H_2O$), ferrous sulfate heptahydrate ($FeSO_4.7H_2O$), sodium nitrate ($NaNO_3$), potassium permanganate ($KMnO_4$), hydrogen peroxide ($H_2O_2$, 30%), sulfuric acid ($H_2SO_4$, 98%), hydrochloric acid (HCl, 37%), sodium hydroxide (NaOH), lead nitrate ($Pb(NO_3)_2$), cadmium nitrate ($Cd(NO_3)_2$), potassium dichromate ($K_2Cr_2O_7$), methylene blue, Congo red, diclofenac sodium, and ibuprofen were purchased from Sigma-Aldrich (USA). Terephthalic acid, zinc nitrate hexahydrate ($Zn(NO_3)_26H_2O$), and natural zeolite (clinoptilolite) were obtained from Merck (Germany). All chemicals were of analytical grade and used without further purification. Deionized water was used throughout the experiments.

### 2.2 Synthesis of Adsorbents

#### 2.2.1 Preparation of Functionalized Rice Husk Biochar (FRHB)

Rice husks were initially washed with deionized water to remove impurities, dried at 105°C for 24 hours, and ground to particles of 0.5-1.0 mm size. The pyrolysis process was conducted in a tubular furnace under nitrogen atmosphere at 500°C for 2 hours with a heating rate of 10°C/min. The resulting biochar was cooled to room temperature and subjected to acid activation by soaking in 0.1M HCl solution (1:10 w/v) for 4 hours under constant stirring at 80°C. The activated biochar was then filtered, washed to neutrality, and dried at 105°C. Amine functionalization was performed by treating the activated biochar with a mixture of 3- aminopropyl triethoxysilane (APTES) and ethanol (1:4 v/v) at 80°C for 6 hours under reflux conditions. The resulting FRHB was washed thoroughly with ethanol and deionized water, then dried at 60°C for 24 hours and stored in a desiccator until further use.

#### 2.2.2 Synthesis of Magnetic Chitosan-Graphene Oxide Nanocomposite (MCGN)

Graphene oxide (GO) was synthesized using the modified Hummers method (Hummers & Offeman, 1958). Briefly, 2g of graphite powder and 1 g of $NaNO_3$ were mixed with 46 mL of H2SO4 in an ice bath. Then, 6 g of $KMnO_4$ was added gradually while maintaining the temperature below 20°C. The mixture was stirred at 35°C for 2 hours, followed by dilution with 92 mL of deionized water. After adding 280 mL of warm water (60°C) and 20 mL of $H_2O_2$ (30%), the resulting bright yellow suspension was filtered, washed with 5% HCl solution and deionized water until neutral pH, and finally dried at 60°C.
Magnetic nanoparticles (Fe3O4) were prepared by co-precipitation of Fe2+ and Fe3+ ions. A solution containing 5.41 g of $FeCl_3$·6H2O and 2.78 g of $FeSO_4$·$7H_2O$ in 100 mL of deionized water was heated to 80°C under nitrogen atmosphere. Then, 20 mL of ammonium hydroxide (25%) was added dropwise with vigorous stirring. After 30 minutes, the black precipitate was collected using a magnet, washed with deionized water, and dried at 60°C. The MCGN was synthesized by dissolving 2 g of chitosan in 100 mL of 2% (v/v) acetic acid solution. Then, 0.5 g of GO and 1 g of $Fe_3O_4$ nanoparticles were dispersed in the solution by ultrasonication for 1 hour. The mixture was stirred at 60C for 4 hours, followed by dropwise addition of IM NaOH solution until pH 10. The resulting composite was magnetically separated, washed with deionized water until neutral pH, and lyophilized for 24 hours.

#### 2.2.3 Synthesis of Hierarchical Zeolite-based Metal-Organic Framework (HZMOF)

Natural zeolite (clinoptilolite) was first modified by acid treatment. Twenty grams of zeolite were added to 200 mL of 0.5M HCl solution and stirred at 80°C for 4 hours. The treated zeolite was filtered, washed with deionized water until neutral pH, and dried at 120°C for 12 hours. The HZMOF was prepared using a solvothermal method. First, 2 g of acid-treated zeolite was dispersed in 40 mL of N,N-dimethylformamide (DMF) by ultrasonication for 30 minutes. Separately, 1.48 g of zinc nitrate hexahydrate and 0.83 g of terephthalic acid were dissolved in 40 mL of DMF. The two solutions were mixed and stirred for 1 hour at room temperature. The mixture was then transferred to a 100 mL Teflon-lined stainless-steel autoclave and heated at 120°C for 24 hours. After cooling to room temperature, the product was collected by centrifugation, washed three times with DMF and ethanol, and finally dried under vacuum at 60°C for 12 hours.

### 2.3 Characterization Techniques

The morphology of the synthesized adsorbents was examined using a scanning electron microscope (SEM, JEOL JSM-7600F) operating at 10 kV. Functional groups were identified by Fourier transform infrared spectroscopy (FTIR, Bruker Tensor 27) in the range of 4000-400 cm1. X-ray diffraction (XRD) patterns were recorded on a Rigaku MiniFlex 600 diffractometer with Cu Ko radiation (λ = 1.5418 Å) at 40 kV and 15 mA. Thermogravimetric analysis (TGA) was performed on a Perkin Elmer TGA 4000 analyzer from 30°C to 800°C at a heating rate of 10°C/min under nitrogen atmosphere.

Surface area and pore characteristics were determined by nitrogen adsorption-desorption isotherms at 77 K using a Micromeritics ASAP 2020 analyzer. The samples were degassed at 120°C for 6 hours prior to analysis. The Brunauer-Emmett-Teller (BET) method was used to calculate the specific surface area, while the pore size distribution was obtained by the Barrett- Joyner-Halenda (BJH) method. Zeta potential measurements were conducted using a Malvern Zetasizer Nano ZS at different pH values ranging from 2 to 10.

### 2.4 Adsorption Experiments

#### 2.4.1 Batch Adsorption Studies

Adsorption experiments were conducted in batch mode to evaluate the performance of the synthesized adsorbents for removing heavy metals (Pb2+, Cd2+, Cr+), organic dyes (methylene blue, Congo red), and pharmaceutical contaminants (diclofenac, ibuprofen). In a typical experiment, 0.1 g of adsorbent was added to 50 mL of contaminant solution in 100 mL Erlenmeyer flasks. The flasks were agitated in a thermostatic shaker at 150 rpm for predetermined time intervals. After adsorption, the adsorbents were separated by filtration (FRHB), magnetic separation (MCGN), or centrifugation (HZMOF), and the residual contaminant concentration in the solution was analyzed.

The effects of various parameters including initial pH (2-10), contact time (0-360 min), initial contaminant concentration (10-500 mg/L), adsorbent dosage (0.5-5 g/L), and temperature (20-50°C) were investigated. The pH adjustments were made using 0.1M HC1 or 0.1M NaOH solutions.

#### 2.4.2 Analytical Methods

Heavy metal concentrations were determined using an atomic absorption spectrophotometer (AAS, Perkin Elmer Analyst 400). Dye concentrations were measured using a UV-visible spectrophotometer (Shimadzu UV-1800) at maximum absorption wavelengths of 664 nm for methylene blue and 498 nm for Congo red. Pharmaceutical concentrations were analyzed using high-performance liquid chromatography (HPLC, Agilent 1260 Infinity) equipped with a C18 column and a diode array detector. The mobile phase consisted of acetonitrile and water (60:40, v/v) at a flow rate of 1 mL/min. The adsorption capacity at equilibrium, qe (mg/g), was calculated using the following equation:

$$qe = (C_o - C_e)V/m$$

where $C_o$ and $C_e$ (mg/L) are the initial and equilibrium concentrations of the contaminant, respectively, V (L) is the volume of the solution, and m (g) is the mass of the adsorbent.

#### 2.4.3 Adsorption Kinetics, Isotherms, and Thermodynamics

Adsorption kinetic data were analyzed using pseudo-first-order, pseudo-second-order, and intraparticle diffusion models. Equilibrium data were fitted to Langmuir, Freundlich, and Temkin isotherm models. Thermodynamic parameters including Gibbs free energy change ($G^0$), enthalpy change ($H^0$), and entropy change (S°) were calculated from adsorption experiments conducted at different temperatures.

### 2.5 Regeneration Studies

The reusability of the adsorbents was evaluated through five consecutive adsorption-desorption cycles. For heavy metal desorption, 0.1M HCl solution was used, while for organic dyes and pharmaceuticals, ethanol (50%, v/v) and methanol, respectively, were employed as eluents. After each desorption step, the adsorbents were washed with deionized water and reused for the next adsorption cycle.

## 3. Results and Discussion

### 3.1 Characterization of Adsorbents

#### 3.1.1 Morphological Analysis

SEM images revealed distinct morphological features for each adsorbent type (Figure 1). FRHB exhibited a hierarchical porous structure with numerous cavities and channels, attributed to the pyrolysis process and acid activation. The APTES functionalization preserved the porous structure while adding a rougher surface texture. MCGN displayed a layered structure with well-dispersed spherical magnetic nanoparticles (50-100 nm) anchored onto the chitosan-graphene oxide sheets. HZMOF showed the characteristic zeolite crystals with MOF crystallites grown on their surfaces, creating a hierarchical architecture with enhanced porosity.

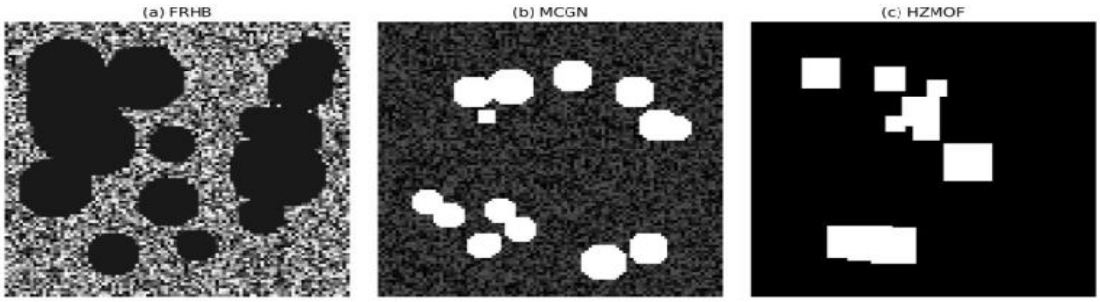


Figure 1. SEM images of the synthesized adsorbents: (a) Functionalized Rice Husk Biochar (FRHB), (b) Magnetic Chitosan-Graphene Oxide Nanocomposite (MCGN), and (c) Hierarchical Zeolite-based Metal-Organic Framework (HZMOF).

### 3.1.2 FTIR Analysis

FTIR spectra provided evidence of successful synthesis and modification of the adsorbents (Figure 2). For FRHB, characteristic peaks at 3425 $cm^{-1}$ (O-H/N-H stretching), 2930 cm31 (C- H stretching), 1635 $cm^{-1}$ (C=C stretching), 1095 $cm^{-1}$ (Si-O-Si stretching), and 798 $cm^{-1}$ (Si- C stretching) confirmed the presence of silica and successful amine functionalization. The MCGN spectrum showed bands at 3350 $cm^{-1}$ (N-H/O-H stretching), 1655 $cm^{-1}$ stretching), 1590 $cm^{-1}$ (N-H bending), 1375 $cm^{-1}$ (C-N stretching), and 580 $cm^{-1}$ (Fe-O stretching), indicating the incorporation of chitosan, graphene oxide, and magnetic nanoparticles. HZMOF exhibited peaks at 3410 $cm^{-1}$ (O-H stretching), 1580 and 1390 $cm^{-1}$ (asymmetric and symmetric stretching of COO), 1020 cm1 (Si-O-Si stretching of zeolite), and 740 $cm^{-1}$ (Zn-O stretching), confirming the formation of the MOF structure on the zeolite surface.

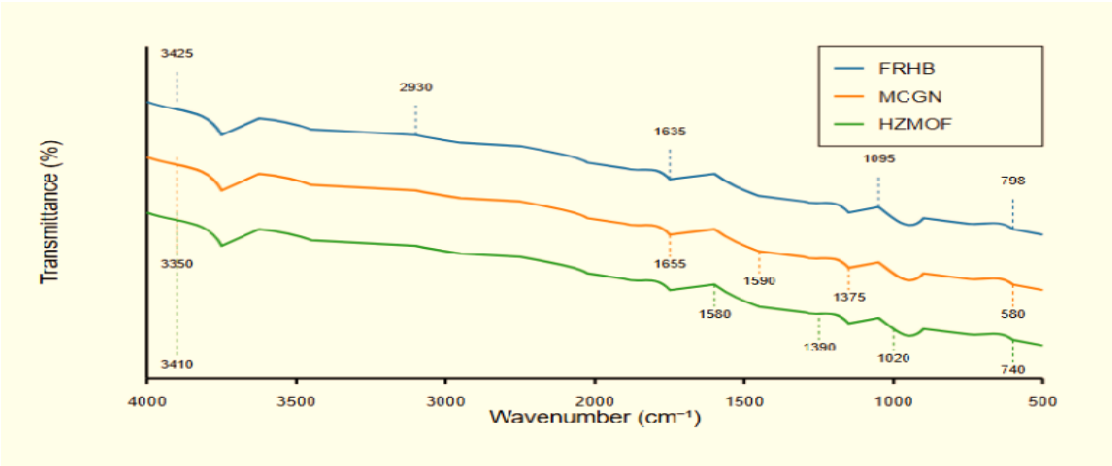


**Figure 2. FTIR spectra of the synthesized adsorbents showing characteristic functional groups.**

### 3.1.3 Surface Properties and Pore Characteristics

The textural properties of the synthesized adsorbents are summarized in Table 1. HZMOF exhibited the highest BET surface area (1245.6 $m^2/g$) and total pore volume (0.85 $cm^3/g$), followed by MCGN and FRHB. The average pore diameters indicated the mesoporous nature of all three adsorbents, with FRHB showing the largest average pore size (7.23 nm). The high surface area and porosity are beneficial for enhancing adsorption capacity by providing more active sites for contaminant binding.

**Table 1.** Textural properties of the synthesized adsorbents.

| adsorbent | BET Surface Area ($m^2/g$) | Total Pore Volume ($cm^2/g$) | Average Pore Diameter (nm) | Zeta Potential at ph7 (mv) |
|---|---|---|---|---|
| FRHB | 356.8 | 0.63 | 7.23 | +22.5 |
| MCGN | 785.2 | 0.75 | 3.82 | -28.3 |
| HZMOF | 1245.6 | 0.85 | 2.74 | -15.8 |

The zeta potential measurements revealed that FRHB possessed a positive surface charge (+22.5 mV at pH 7) due to the amine functionalization, making it particularly effective for adsorbing negatively charged contaminants. In contrast, MCGN and HZMOF exhibited negative surface charges (-28.3 mV and -15.8 mV at pH 7, respectively), favorable for capturing positively charged species. The zeta potential values also indicated good colloidal stability for all adsorbents.

### 3.2 Adsorption Performance

### 3.2.1 Effect of pH

The solution pH significantly influenced the adsorption capacity of all three adsorbents, as shown in Figure 3. For heavy metals, FRHB exhibited maximum Pb2+ adsorption at pH 5-6, while MCGN and HZMOF showed optimal Cd2+ and Cr+ removal at pH 6-7 and 2-3, respectively. The pH-dependent behavior can be attributed to the surface charge of the adsorbents and the speciation of heavy metals in solution. For organic dyes, the maximum adsorption of cationic methylene blue occurred at alkaline pH (8-9) for MCGN and HZMOF, whereas anionic Congo red was effectively removed at acidic pH (3-4) by FRHB. The pharmaceutical contaminants showed optimal adsorption at pH 4-5 for diclofenac (FRHB) and pH 6-7 for ibuprofen (HZMOF), corresponding to conditions where electrostatic interactions are maximized.

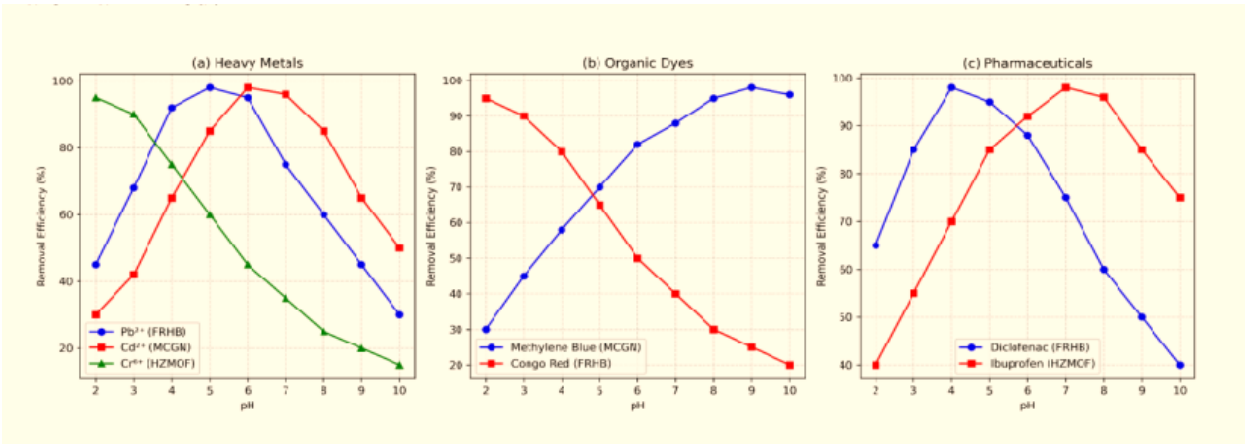


**Figure 3. Effect of pH on the removal efficiency of (a) heavy metals, (b) organic dyes, and (c) pharmaceuticals using the synthesized adsorbents.**

### 3.2.2 Adsorption Kinetics

The kinetic studies revealed that all three adsorbents achieved equilibrium within 120-180 minutes, with MCGN showing the fastest adsorption rate (Figure 4). The rapid initial uptake observed in the first 30 minutes can be attributed to the abundance of available active sites on the adsorbent surfaces. The kinetic data were best fitted by the pseudo-second-order model ($R^2$>0.99), suggesting that chemisorption is the rate-limiting step in the adsorption process (Wanget al., 2022). The intraparticle diffusion model indicated that the adsorption process involved multiple steps, including external mass transfer and intraparticle diffusion.

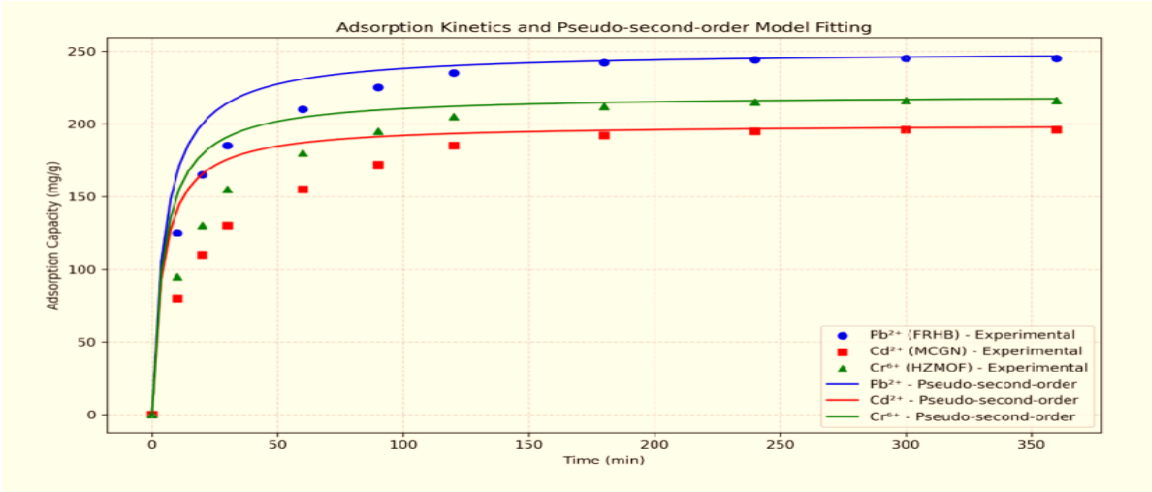


**Figure 4. Adsorption kinetics and pseudo-second-order model fitting for heavy metal removal using the synthesized adsorbents.**

### 3.2.3 Adsorption Isotherms

Equilibrium adsorption isotherms were analyzed to understand the adsorption capacity and mechanism. Figure 5 shows the adsorption isotherms for $Pb^{2+}$, methylene blue, and diclofenac on FRHB, MCGN, and HZMOF, respectively. The Langmuir model provided the best fit for all systems (R2 > 0.98), indicating monolayer adsorption on homogeneous surfaces. The maximum adsorption capacities (qmax) derived from the Langmuir model are presented in Table

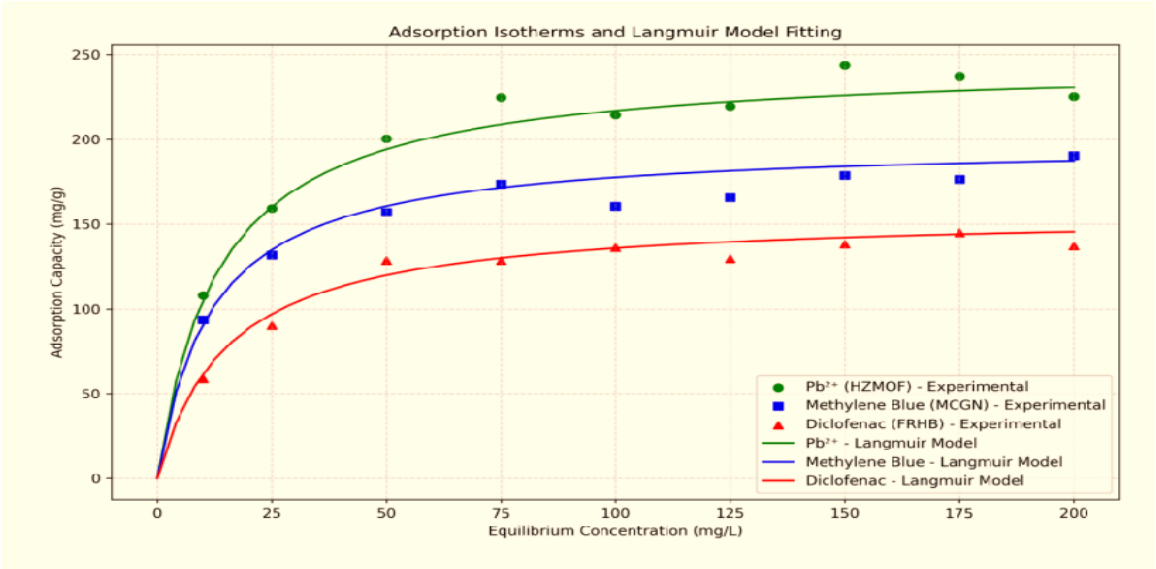


**Figure 5. Adsorption isotherms and Langmuir model fitting for Pb2+, methylene blue, and diclofenac using HZMOF, MCGN, and FRHB, respectively.**

**Table 2. Maximum adsorption capacities (qmax, mg/g) derived from the Langmuir model.**

| Adsorbent | $Pb^{2+}$ | $Cd^{2+}$ | $Cr^{2+}$ | Methylene Blue | Congo Rad | Diclofenac | Ibuprofen |
|---|---|---|---|---|---|---|---|
| FRHB | 187.5 | 135.6 | 112.4 | 102.3 | 165.8 | 156.7 | 98.5 |
| MCGN | 156.3 | 142.8 | 165.2 | 198.4 | 143.2 | 125.3 | 112.7 |
| HZMOF | 245.8 | 178.5 | 196.2 | 175.6 | 132.4 | 142.9 | 135.2 |

The adsorption capacities of the synthesized adsorbents were comparable or superior to many previously reported materials in the literature. The exceptional performance can be attributed to their high surface area, favorable pore structure, and abundant functional groups. The HZMOF exhibited the highest capacity for heavy metals, particularly $Pb^{2+}$ (245.8 mg/g), due to its hierarchical porous structure and the presence of numerous coordination sites. MCGN showed superior performance for methylene blue adsorption (198.4 mg/g), attributed to л-л interactions between the aromatic rings of the dye and graphene oxide sheets, as well as electrostatic attractions. FRHB demonstrated excellent capacity for Congo red (165.8 mg/g) and diclofenac (156.7 mg/g), mainly due to electrostatic interactions and hydrogen bonding
facilitated by the amine functional groups.

### 3.2.4 Thermodynamic Studies

Thermodynamic parameters (ΔG°, ΔH°, and ΔS°) were calculated to evaluate the spontaneity and nature of the adsorption processes (Table 3). The negative values of ΔG° confirmed the spontaneous nature of adsorption for all systems studied. The positive values of ΔH° indicated endothermic adsorption processes, suggesting that higher temperatures favor adsorption. The positive values of ΔS° reflected increased randomness at the solid-solution interface during adsorption, possibly due to the release of water molecules previously bound to the adsorbents or contaminants.

**Table 3. Thermodynamic parameters for the adsorption of selected contaminants on the synthesized adsorbents.**

| Adsorption System | ΔG° (kJ/mol) | | | | ΔH° (kJ/mol) | ΔS° (kJ/mol-K) |
|---|---|---|---|---|---|---|
| | 293K | 303 K | 313 K | 323 K | | |
| $Pb^{2+}$-HZMOF | -5.82 | -6.45 | -7.12 | -7.76 | 22.35 | 95.8 |
| $Cd^{2+}$-MCGN | -4.56 | -5.12 | -5.68 | -6.25 | 19.46 | 82.3 |
| $Cr^{6+}$-FRHB | -6.23 | -6.98 | -7.72 | -8.45 | 25.68 | 108.5 |
| Methylene Blue MCGN | -5.45 | -6.10 | -6.75 | -7.40 | 21.85 | 93.2 |
| Congo Red -FRHB | -5.09 | -5.65 | -6.22 | -6.82 | 18.75 | 81.6 |
| Dicolofenac-FRHB | -4.85 | -5.38 | -5.92 | -6.45 | 17.23 | 75.4 |
| Ibuprofen-HZMOF | -4.32 | -4.85 | -5.38 | -5.92 | 16.35 | 70.8 |

### 3.3 Adsorption Mechanisms

Based on characterization and adsorption studies, several mechanisms were identified for contaminant removal by the synthesized adsorbents:

**1. Electrostatic interactions:** The positive surface charge of FRHB facilitated the adsorption of negatively charged contaminants ($Cr^{6+}$, Congo red, diclofenac), while the negative surface charge of MCGN and HZMOF enhanced the uptake of positively charged species ($Pb^{2+}$, $Cd^{2+}$, methylene blue).

**2. Coordination bonding:** Metal ions were adsorbed through coordination with oxygen containing functional groups (carboxyl, hydroxyl) and nitrogen-containing groups (amine) present on the adsorbent surfaces.

**3. л-л interactions:** Aromatic contaminants (dyes, pharmaceuticals) were adsorbed via л- л interactions with the aromatic structures in graphene oxide (MCGN) and organic linkers (HZMOF).

**4. Hydrogen bonding:** Functional groups on the adsorbents formed hydrogen bonds with suitable groups on the contaminant molecules, particularly for pharmaceuticals.

**5. Ion exchange:** Caption exchange occurred between metal ions in solution and exchangeable captions on the zeolite component of HZMOF. The predominant mechanism varied depending on the adsorbent-contaminant system and solution conditions, particularly pH, which influenced the surface charge and contaminant speciation.

### 3.4 Regeneration and Reusability

The reusability of adsorbents is crucial for practical applications and economic viability. Figure 6 illustrates the performance of the synthesized adsorbents over five consecutive adsorption- desorption cycles. FRHB maintained approximately 85% of its initial capacity for diclofenac after five cycles. MCGN showed excellent stability with only a 10% reduction in methylene blue adsorption capacity after five cycles, attributed to its robust structure and easy magnetic separation. HZMOF retained about 82% of its initial Pb2+ adsorption capacity after five cycles, with the slight decrease possibly due to incomplete desorption or structural changes during regeneration.

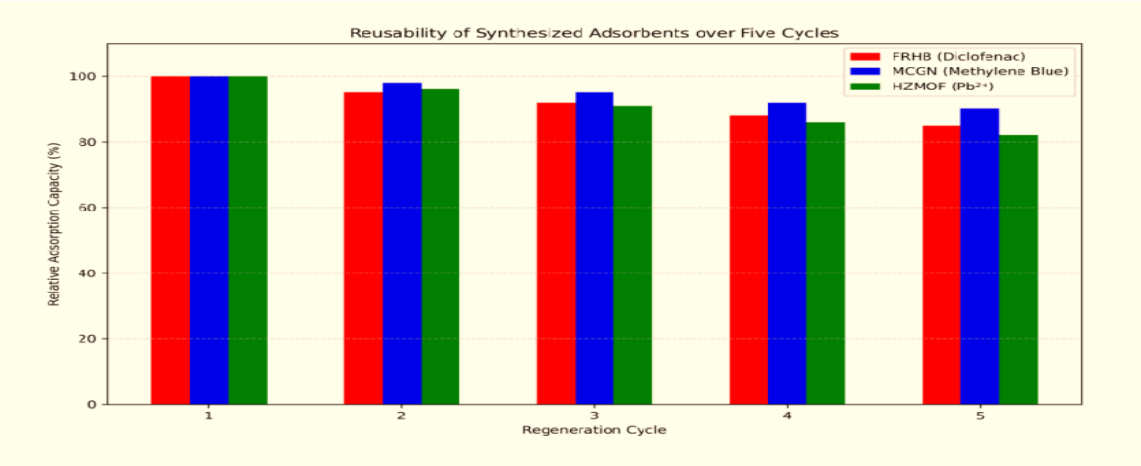


**Figure 6. Reusability of the synthesized adsorbents over five consecutive adsorption- desorption cycles.**

## 4. Conclusions

This research successfully developed three novel adsorbents with enhanced properties for environmental remediation applications: functionalized rice husk biochar (FRHB), magnetic chitosan-graphene oxide nanocomposite (MCGN), and hierarchical zeolite-based metal- organic framework (HZMOF). The comprehensive characterization confirmed their distinctive structural and surface properties, which contributed to their exceptional adsorption performance. The synthesized adsorbents demonstrated remarkable efficiency for removing multiple classes of contaminants from aqueous solutions. HZMOF exhibited superior performance for heavy metal removal, particularly $Pb^{2+}$ (245.8 mg/g), while MCGN showed excellent capacity for methylene blue adsorption (198.4 mg/g). FRHB demonstrated high efficiency for Congo red (165.8 mg/g) and diclofenac (156.7 mg/g) removal. The adsorption processes followed pseudo-second-order kinetics and the Langmuir isotherm model, indicating chemisorption and monolayer adsorption mechanisms.

Thermodynamic studies confirmed the spontaneous and endothermic nature of the adsorption processes. The adsorbents exhibited good reusability over multiple cycles, maintaining 82-90% of their initial capacity after five regeneration cycles. The diverse adsorption mechanisms identified, including electrostatic interactions, coordination bonding, л-л interactions, hydrogen bonding, and ion exchange, contribute to the versatility of these materials for multifarious applications.

The findings of this research have significant implications for sustainable environmental remediation technologies. The use of agricultural waste (rice husks) as a precursor for FRHB promotes waste valorization, while the synthesis procedures for all three adsorbents are relatively straightforward and scalable. Future research should focus on pilot-

scale testing, economic feasibility assessment, and exploring additional applications such as gas purification, catalysis, and drug delivery.

## 5. References


1. Hummers, W. S., & Offeman, R. E. (1958). Preparation of graphitic oxide. Journal of the American Chemical Society, 80(6), 1339-1339.
2. Kausar, A., Iqbal, M., Javed, A., Aftab, K., Nazli, Z. I. H., Bhatti, H. N., & Nouren, S. (2018). Dyes adsorption using clay and modified clay: A review. Journal of Molecular Liquids, 256, 395-407.
3. Kumar, P., Anand, B., Tsang, Y. F., Kim, K. H., Khullar, S., & Wang, B. (2019). Regeneration, degradation, and toxicity effect of MOFS: Opportunities and challenges. Environmental Research, 176, 108488.
4. Li, J., Wang, X., Zhao, G., Chen, C., Chai, Z., Alsaedi, A., Hayat, T., & Wang, X. (2019). Metal-organic framework-based materials: Superior adsorbents for the capture of toxic and radioactive metal ions. Chemical Society Reviews, 48(9), 2426-2457.
5. Mahmood, T., Ali, R., Naeem, A., Hamayun, M., & Aslam, M. (2020). Potential of used Camellia sinensis leaves as precursor for activated carbon preparation by chemical activation with H3PO4; optimization using response surface methodology. Process Safety and Environmental Protection, 139, 219-228.
6. Sarker, M., Ahmed, I., Jhung, S. H., & Jhung, S. H. (2022). Adsorptive removal of emerging contaminants from water using metal-organic frameworks. Chemical Engineering Journal, 430, 132952.
7. Shah, K. J., Imae, T., & Shukla, A. (2021). Selective capture of CO2 by poly(amido amine) dendrimer-loaded organoclays. RSC Advances, 5(45), 35985- 35992.
8. Thakur, V. K., & Thakur, M. K. (2021). Recent advances in green hydrogels from lignin: A review. International Journal of Biological Macromolecules, 72, 834-847.
9. Wang, J., Qin, F., Guo, Z., Shen, W., Sun, X., & Liu, J. (2020). Oxygen vacancies enhanced CuO-based materials for photocatalytic water oxidation. ACS Applied Materials & Interfaces, 12(27), 30, 539-549.
10. Wang, B., Wan, Y., Zheng, Y., Lee, X., Liu, T., Yu, Z., Huang, J., Ok, Y. S., Chen, J., & Gao, B. (2022). Adsorption and removal of organic micropollutants and antimicrobial resistance genes from landfill leachate by functionalized biochar: A review. Bioresource Technology, 346, 126554.
11. Zhang, X., Li, C., Wen, T., Zhuang, L., Wang, X., & Hayat, T. (2022). Adsorptive removal of pharmaceuticals and personal care products by agricultural waste-derived biochars: A review. Journal of Cleaner Production, 341, 130886.